Numerical Analysis on Added Resistance of Ships in Time-domain

Kyong-Hwan Kim*, Soizic Joncquez, Yonghwan Kim*, Harry Bingham*****
*Seoul National University, Seoul, Korea
** FORCE Technology, Lyngby, Denmark
*** Technical University of Denmark, Lyngby, Denmark

1. Introduction

Accurate prediction of added resistance on ships is one of crucial elements for power prediction, since the magnitude of added resistance can be 10~30 % of calm-water wave resistance. There are two major analytical approaches to estimate added resistance due to waves. One is a far-field method based on the momentum-conservation theory proposed by Maruo (1960), and the other approach is a near-field method by integrating pressures on the body surface. For many past years, the former approach has been widely applied due to its simplicity and efficiency, which has no need to compute hydrodynamic pressure on the complicated body surface. Recently, thanks to growing up of computer technology, the near-field method is being acclaimed as an alternative method. In the near-field method, the wave Green function method has been applied in frequency domain. Very recently, Joncquez et al.(2008, 2009) solved the added resistance by using a ship motion program, AEGIR, and they compared the results between momentum-conservation approach and direct pressure integration. Furthermore, computational results based on Neumann-Kelvin and double-body linearization schemes were compared.

In the present study, the two time-domain Rankine panel methods are applied for the computation of added resistance, and their results are compared. The computer programs to be considered are AEGIR and WISH. Details about the added-resistance computation by extending AEGIR can be found in the works of Joncquez et al.(2008, 2009). In the case of WISH developed by Kim et al.(2007), there are some differences of formulation and numerical methods, but there are many similarity such as the adoption of Rankine panel method, time-domain approach, and B-spline basis function.

The present study includes the comparison of the two linearization schemes: Neumann-Kelvin(NK) and double-body(DB) linearizations. Computed quantities of added resistance are validated for a few ships models, including Wigley hulls, Series 60 (C_B=0.7) and S175 containership by comparing with experimental data. Furthermore, the components of added resistance are observed for each integral term, and the contributions of radiation and diffraction components are also compared.

2. Theoretical background

2.1 Boundary Value Problem

The adoption of potential theory is a typical approach to tackle the ship motion problem. When a ship, advancing a constant speed U, is under wave excitation, the boundary value problem for velocity potential (ϕ) can be formulated as follows:

$$\nabla^2\phi = 0 \qquad in\ fluid\ domain \tag{1}$$

$$\frac{\partial\phi}{\partial n} = \vec{U}\cdot\vec{n} + \frac{\partial\vec{\delta}}{\partial t}\cdot\vec{n} \quad on\ S_B \tag{2}$$

$$\left[\frac{d}{dt} + \nabla\phi\cdot\nabla\right]\left[z-\zeta(x,y,t)\right] = 0 \quad on\ z=\zeta(x,y,t) \tag{3}$$

$$\frac{d\phi}{dt} = -g\zeta - \frac{1}{2}\nabla\phi\cdot\nabla\phi \qquad on\ z=\zeta(x,y,t) \tag{4}$$

where $\frac{d}{dt} = \frac{\partial}{\partial t} - \vec{U}\cdot\nabla$. In addition, ζ and g are wave elevation and gravity constant, respectively. The boundary value problem can be linearized by decomposing the total velocity potential as follows:

$$\phi(\vec{x},t) = \Phi(\vec{x}) + \phi_I(\vec{x},t) + \phi_d(\vec{x},t) \tag{5}$$

$$\zeta(\vec{x},t) = \zeta_I(\vec{x},t) + \zeta_d(\vec{x},t) \tag{6}$$

Φ indicates the basis potential, and the subscript I and d indicates the incident and disturbed component for potential and elevation. The linearized boundary conditions take the following forms:

$$\left[\frac{\partial}{\partial t} - (\vec{U}-\nabla\Phi)\cdot\nabla\right]\zeta_d = \frac{\partial^2\Phi}{\partial z^2}\zeta_d + \frac{\partial\phi_d}{\partial z} + (\vec{U}-\nabla\Phi)\cdot\nabla\zeta_I \tag{7}$$

$$\left[\frac{\partial}{\partial t} - (\vec{U}-\nabla\Phi)\cdot\nabla\right]\phi_d = -g\zeta_d + \left[\vec{U}\cdot\nabla\Phi - \frac{1}{2}\nabla\Phi\cdot\nabla\Phi\right] + (\vec{U}-\nabla\Phi)\cdot\nabla\phi_I \tag{8}$$

$$\frac{\partial \phi_d}{\partial n} = \sum_{j=1}^{6}\left(\frac{\partial \xi_j}{\partial t} n_j + \xi_j m_j\right) - \frac{\partial \phi_I}{\partial n} \qquad on\ \bar{S}_B$$
$$(m_1, m_2, m_3) = (\vec{n}\cdot\nabla)(\vec{U} - \nabla\Phi) \tag{9}$$
$$(m_4, m_5, m_6) = (\vec{n}\cdot\nabla)(\vec{x}\times(\vec{U} - \nabla\Phi))$$

where, m_i is m-term which contains an interaction term between the steady and unsteady solutions. The Eqs. (7)~(9) are the boundary conditions for double-body linearization when Φ takes the double-body flow potential. By substituting Φ by zero in Eqs. (7)~(9), the boundary value problem of Neumann-Kelvin linearization can be provided.

The ship motion can be obtained by solving an equation of motion as follow:

$$[M]\{\ddot{\xi}\} + [C]\{\xi\} = \{F_{F.K.}\} + \{F_{H.D.}\} \tag{10}$$

$[M]$ is the mass matrix of ship. $\{F_{F.K.}\}$, and $\{F_{H.D.}\}$ are Froude-Krylov and hydrodynamic forces, respectively. Details of numerical implementations about the boundary value problem and the equation of motion are found in Kim et al.(2007).

2.2 Formulation of Added Resistance

By using Bernoulli's equation and Taylor's expansion, the second-order pressure can be evaluated, and the second-order force is provided by integrating the second-order pressure on the body surface. The added resistance can be obtained by averaging the second-order force signal as follow:

$$\begin{aligned}
\overline{F_2} &= \int_{WL} \frac{1}{2}\rho g(\eta - z_1)^2 \cdot \vec{n}\, dL \\
&- \rho \int_{WL} \left\{-U\frac{\partial \Phi}{\partial x} + \frac{1}{2}\nabla\Phi\cdot\nabla\Phi\right\}(\eta - z_1)\cdot\vec{n}_1\, dL \\
&- \rho \int_{WL} (\vec{X}_1\cdot\nabla)\left\{-U\frac{\partial \Phi}{\partial x} + \frac{1}{2}\nabla\Phi\cdot\nabla\Phi\right\}(\eta - z_1)\cdot\vec{n}\, dL \\
&- \rho\iint_{\bar{S}_B} g z_0\cdot\vec{n}_2\, ds - \rho\iint_{\bar{S}_B}\left(g z_1 + \frac{\partial \phi_1}{\partial t} - U\frac{\partial \phi_1}{\partial x} + \nabla\Phi\cdot\nabla\phi_1\right)\cdot\vec{n}_1\, ds \\
&- \rho\iint_{\bar{S}_B}\left\{\frac{1}{2}(\nabla\phi_1\cdot\nabla\phi_1)\cdot\vec{n}\right\} ds \\
&- \rho\iint_{\bar{S}_B}\vec{X}_1\cdot\nabla\left(\frac{\partial \phi_1}{\partial t} - U\frac{\partial \phi_1}{\partial x} + \nabla\Phi\cdot\nabla\phi_1\right)\cdot\vec{n}\, ds \\
&- \rho\iint_{\bar{S}_B}\left[\left\{-U\frac{\partial \Phi}{\partial x} + \frac{1}{2}\nabla\Phi\cdot\nabla\Phi\right\}\cdot\vec{n}_2\right] ds \\
&- \rho\iint_{\bar{S}_B}\vec{X}_1\cdot\nabla\left\{-U\frac{\partial \Phi}{\partial x} + \frac{1}{2}\nabla\Phi\cdot\nabla\Phi\right\}\cdot\vec{n}_1\, ds
\end{aligned} \tag{11}$$

In order to obtain the added resistance, it is no need to solve the second-order boundary value problem because a mean value of the second-order velocity potential is zero. Added resistance can be obtained also by using a momentum approach. The details on the momentum approach can be found in the work of Joncquez(2009).

3. Analysis Results

Two Wigley hull models, Series 60(C_B =0.7) and S175 containership are considered for numerical analysis. The principal dimension of the test models are appeared in Table 1, and panel models are shown in Fig. 1.

Table 1 Principal dimension of the test models(m)

Model	Wigley I	Wigley III	Series 60	S175
L	3.0	3.0	100.0	175.0
B/L	0.1	0.1	0.143	0.145
D/L	0.0625	0.0625	0.057	0.054
C_B	0.560	0.462	0.7	0.561

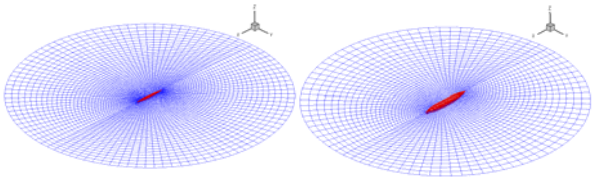

(a) Wigley model (b) Series 60 (C_B=0.7) hull

Fig. 1 Hydrodynamic panel models of the test models

Fig. 2 shows disturbed wave patterns around of Series 60. Nakos(1990) compared the steady wave elevations computed by the Neumann-Kelvin and double-body linearizations with the existing experiment data, and he pointed out that major differences are found in near bow and stern regions. In the present study, the same conclusion is found.

Linear and the second-order forces on Wigley I model with Fn=0.2 are shown in Fig. 3. The second-order force contains only the quadratic components of linear solutions, as appeared in Eq. (11). The second-order force oscillates two times faster than the linear force, as expected. Added resistance is the mean value of this second-order force.

Figs. 4 and 5 show added resistances of Wigley hull I model at Fn=0.2 and 0.3 with respect to the wave length. At Fn=0.2, there are no big difference between the results of the Neumann-Kelvin and double-body linearizations, and the computational results show favorable agreements with experimental data. At Fn=0.3, the magnitude of added resistance between the two linearization schemes are similar, however the resonance frequency of the Neumann-Kelvin linearization is closer to experimental data than the double-body linearization. In fact, the double-body linearization is a slow-ship approach, and this means

that the accuracy of computational results by the double-body linearization can be poorer as ship goes faster. Therefore, it is reasonable that the results of the double-body linearization show good correspondence at Fn=0.2, while a little differences are found at Fn=0.3 as shown in Figs 4 and 5. At high Froude numbers, The Neumann-Kelvin linearization is recommended rather than the double-body linearization.

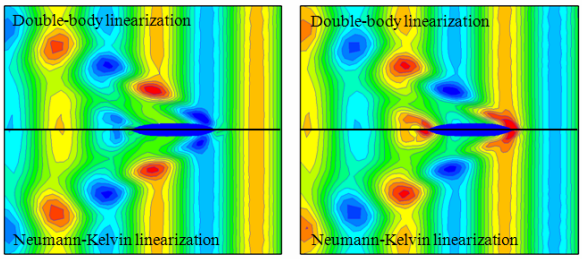

(a) $T\sqrt{g/L} = 34.43$ (b) $T\sqrt{g/L} = 40.69$

Fig. 2 Added Resistance of Series 60 hull: Fn=0.222, wave heading angle = 180 deg, λ/L=1.136

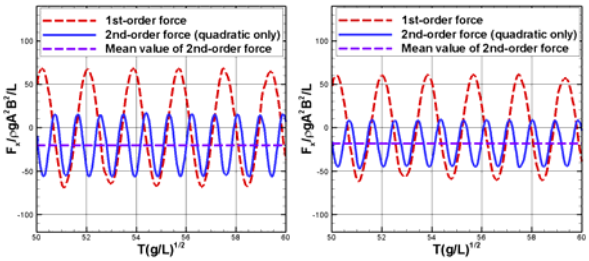

(a) Neumann-Kelvin (b) Double-body

Fig. 3 Time-histories of surge force on Wigley I hull: Fn=0.2, wave heading angle = 180 deg, λ/L=1.15

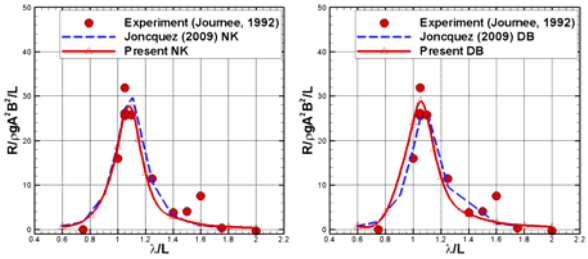

(a) Neumann-Kelvin (b) Double-body

Fig. 4 Added resistance of Wigley I hull: Fn = 0.2, wave heading angle = 180 deg

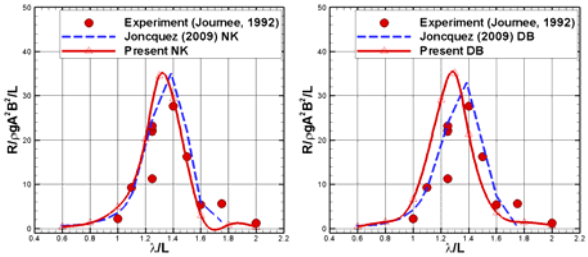

(a) Neumann-Kelvin (b) Double-body

Fig. 5 Added resistance of Wigley I hull: Fn = 0.3, wave heading angle = 180 deg

The added resistance of Series 60(C_B=0.7) with Fn=0.222 is shown in Fig. 6. The results of the double-body approach show better agreement with the experimental data than those of the Neumann-Kelvin linearization. The fundamental assumption of the Neumann-Kelvin linearization comes from the thin-ship theory that beam-to-length ratio is small, therefore in case of Series 60 which has larger beam-to-length than Wigley hull model, the double-body linearization seems more reasonable rather than the Neumann-Kelvin linearization.

In the case of Wigley I model, the results of Joncquez(2009) shows better agreement with measured data at Fn=0.3. On the other hand, in the case of Series 60, the results of WISH show better prediction. In order to investigate the reason of different tendencies between the results of WISH and AEGIR, a comparative study on the linear solutions should be done more thoroughly.

The added resistance of S175 containership is shown in Fig. 7. At high Froude number, discrepancy between the results of two linearization schemes is large. The results of double-body linearization show better correspondences with the experimental data than the results of the Neumann-Kelvin linearization.

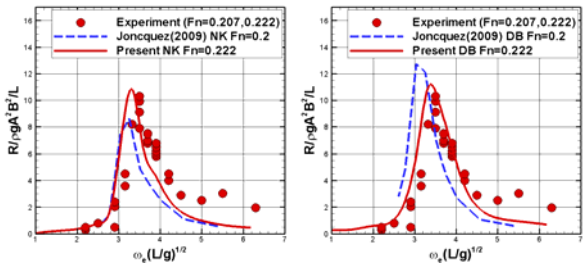

(a) Neumann-Kelvin (b) Double-body

Fig. 6 Added resistance of Series 60 hull: wave heading angle = 180 deg

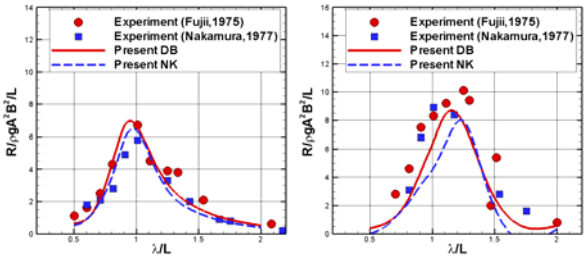

(a) Fn=0.15 (b) Fn=0.25

Fig. 7 Added resistance of S157 containership: wave heading angle = 180 deg

Global agreements between the computational results and measured data are described in Table 1. The agreement is presented in three levels: very good (◯), good(△) and bad(X). At low Froude number, both linearization schemes show good correspondences with experimental data. Overall, the Neumann-Kelvin

linearization shows better agreement than the double-body linearization at high Froude number. In the cases of Wigley hulls considered as thin ships, the Neumann-Kelvin linearization shows better prediction than the double-body linearization, while in the case of Series 60 and S175 containership, fatter than Wigley hulls, the double-body linearization shows better solutions than the Neumann-Kelvin linearization. All of these tendencies are natural according to the fundamental assumptions of the two linearization schemes.

Table 2 Agreement between computational results and experimental data (○: very good, △: good, X:bad)

Fn	Wigley I		Wigley III		Series 60		S175	
	NK	DB	NK	DB	NK	DB	NK	DB
0.15	-	-	-	-	-	-	○	○
0.2	○	○	△	△	△	○	△	○
0.25	-	-	-	-	-	-	X	△
0.3	△	X	△	X	-	-	X	X

The components of added resistance on S175 containership are shown in Fig. 8. (I) is waterline integral term, and (II) to (V) are each integral term as appeared in Eq. (11), (VI) is last two integral terms. It is easily found that the most dominant component of the added resistance is (I). (III) or (V) also takes significant amount. It means that the radiation component is important when the wave length is comparable with ship length. These are clearly appeared in Fig. 8-(b). The radiation component is much larger than the diffraction component in near resonance-wave length.

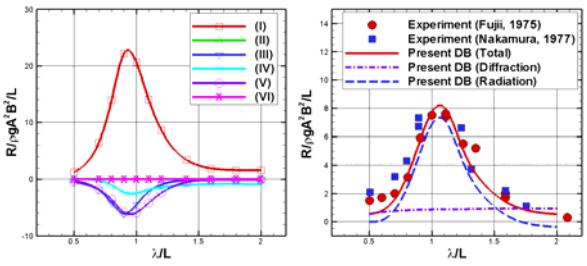

(a) Integral term (b) Radiation and diffraction

Fig. 8 Components of added resistance on S175 containership: Fn=0.2, wave heading angle = 180 deg

In short or long waves away from the resonance-wave length, the diffraction component is larger than the radiation component. This trend was already well known, and it is appeared in the range of $\lambda/L<0.8$.

4. Conclusions

The added resistance of ship is handled with a B-spline-based Rankine panel method in time domain. Added resistance values computed by using the both Neumann-Kelvin and double-body linearizations are compared each other as well as with experimental data for Wigley hulls, Series 60 hull, and S175 containership, showing reasonable agreement. Computational results by using the Neumann-Kelvin linearization show better correspondence with experimental data at high Froude numbers and for thin ships with small beam-to-length ratios, while those of the double-body linearization seem to provide better agreement at low Froude numbers and for fat displacement ships. Therefore proper linearization scheme should be applied, depending on ship speed and hull form.

References

- Dawson, C.W., 1977, "A practical computer method for solving ship-wave problem", 2nd Numerical Ship Hydrodynamics, 30-38.
- Joncquez, S.A.G., Bingham, H., Andersen, P., 2008, "Validation of added resistance computations by a potential flow boundary element method", 27th Naval Hydrodynamics, Seoul, Korea.
- Joncquez, S.A.G., 2009, Second-Order Forces and Moments Acting on Ships in Waves, PhD Thesis, Technical University of Denmark.
- Joncquez, S.A.G., Bingham, H., Andersen, P., 2009, "A comparison of methods for computing the added resistance of ships using a higher-order BEM", 24th IWWWFB, 121-124.
- Kim, K.H., Kim, Y., Kim, Y., 2007, WISH JIP project report and manual, Marine Hydrodynamic Laboratory, Seoul National University.
- Maruo, H., 1960, "The drift of a body floating on waves", Journal of Ship Research 4(3), 1-10.
- Nakos, D.E., 1990, Ship wave patterns and motions by a three dimensional Rankine panel method, PhD Thesis, MIT, Cambridge, MA.